https://doi.org/10.18321/ectj1080

Ni/Cr-[α-$SiW_{12}O_{40}$] Layered Double Hydroxide as Effective Adsorbent of Iron(II) From Aqueous Solution

A. Lesbani[1,2]*, M.F. Azmi[2], N.R. Palapa[1], T. Taher[2], R. Andreas[3], R. Mohadi[1,2]

[1]Graduate School of Mathematics and Natural Sciences, Faculty of Mathematics and Natural Sciences, Universitas Sriwijaya, Jl. Palembang Prabumulih Km. 32 Ogan Ilir 30662, Indonesia
[2] Research Center of Inorganic Materials and Coordination Complexes, Faculty of Mathematics and Natural Sciences, Universitas Sriwijaya, Jl. Palembang Prabumulih Km. 32 Ogan Ilir 30662, Indonesia
[3]Department of Chemistry, Faculty of Mathematics and Natural Sciences, Universitas Jenderal Soedirman, Jl. Dr. Soeparno, Karangwangkal, Purwokerto Utara, Banyumas, 53123, Indonesia

Article info

Received:
9 November 2020

Received in revised form:
6 January 2021

Accepted:
16 March 2021

Abstract

Layered double hydroxide (LDH) Ni/Cr intercalated [α-$SiW_{12}O_{40}$]$^{4-}$ has been prepared using the coprecipitation method. Materials were characterized by X-ray, FTIR, BET, and pHpzc analyses. Material Ni/Cr-[α-$SiW_{12}O_{40}$] LDHs exhibited a high surface area 98.986 m^2 g^{-1} from 11.030 m^2 g^{-1} for Ni/Cr LDH where the interlayer space was an increase from 7.99 to 10.87 Å with indicated that high crystallinity. Ni/Cr-[α-$SiW_{12}O_{40}$] LDHs showed higher adsorption capacity for iron(II) is up to 250 mg g^{-1}. Adsorption of iron(II) on LDHs has an endothermic process and classify as physical adsorption.

1. Introduction

Wastewater treatment is an important universal concern due to environmental impact and human health [1]. Wastewater is produced on a large and small scale from industry and domestic activities containing heavy metals and dyes [2]. The widest pollutants in wastewater are heavy metals. Heavy metals have a bad effects on the environmental and humans because heavy metals ion can be accumulated in the organism [3], so these problems are challenging researchers to overcome the heavy metal bad effect on the environmental. Various materials have been developed as adsorbents of heavy metals including organic and inorganic adsorbents [4, 5]. Organic adsorbents such as cellulose, lignin, chitin, chitosan, and algae have been used to remove heavy metals from wastewater [6–8]. On the other hand, inorganic adsorbents such as zeolite, activated carbon, clay, bentonite, montmorillonite, and also synthetic layer materials have been widely applied to remove heavy metal from aqueous solution [9–11].

*Corresponding author.
E-mail: aldeslesbani@pps.unsri.ac.id

Synthetic layer materials are well-known as layered double hydroxide (LDH). LDH is hydrotalcite-like materials contains M^{2+}/M^{3+} metal ions and anion between interlayer space of LDH [12]. The anion of LDH can be found as nitrate, carbonate, sulfate, and also chloride depending on the synthetic precursor of materials. The general formula of LDH is $[M^{2+}_{1-x}M^{3+}_{x}(OH)_2]^{x+}(An^-)_{x/n}]nH_2O$ where M^{2+} is divalent, and M^{3+} is trivalent metal ions and An^- is interlayer anions with valence n [13]. A combination of M^{2+} with M^{3+} resulted in various kinds of LDH with unique physical and chemical properties [14].

LDH was applied in wide range of applications, including as an adsorbent of heavy metal ions. LDH of Zn/Al has been tested as a selective adsorbent for removal In^{3+} ion metal ion mixtures from aqueous solution [15]. As present by previous research, NiAl LDH which has been reported the adsorption capacity of Cu(II) removal is 60 mg/g at pH 5 and 298 K. MoS_4-LDH towards Ag^+ ion have been studied by Ma [16]. The adsorption process was carried out by pH 5.9 and obtained an adsorption capacity 8.2 mg/g. Bin Ou et al. [17] reported that CoFe LDH has been examined to remove Cr(VI)

from aqueous solution. The adsorption process obtained adsorption capacity at equilibrium after 90 min is 33.5 mg/g. LDH nanosheets were used to remove Cr(VI) ion from aqueous solution with the fast process due to interaction such as electrostatic attraction, ion exchange, and hydrogen bonding between the metal ion and adsorbent [18]. On the other hand, LDH can be modified by intercalation and impregnation with other materials to increase the physical properties of the LDH such as surface area, structure stability, resistance to acid and also enhanced adsorption ability. The modification of LDH was widely conducted by various methods such as intercalation with anionic compounds, coating with metal oxide, composite and nanocomposite with several compounds.

Efficient adsorption of Mn(II) was achieved by Mg/Al LDH intercalated with diethylenetriaminepentaacetic acid [19]. The adsorption mechanism occurred between the carboxyl group of intercalant with the hydroxyl group of LDH, which was bind with manganese ion. Zn/Al LDH was also intercalated with thiacalix[4]arane anion by calcination/restoration into LDH. These materials were used as adsorbents of Pb^{2+} and Cu^{2+} with adsorption capacity (qm) for Pb^{2+} and Cu^{2+} up to 217 mg g^{-1} and 125 mg g^{-1}, respectively [20]. As reported by Oktrianty et al., [21] ZnCr LDHs intercalated with Keggin ion [α-$SiW_{12}O_{40}$]$^{4-}$ has higher adsorption capacity (76.9 mg/g) than ZnCr LDHs without intercalation (45.4 mg/g). On the other hand, modified zeolites and sands coated with Zn/Al LDH have a selective binding with cadmium in the existence of several ions such as K^+, NH^{4+}, NO_3-, and HPO_4^{2-} [22]. Ca/Al LDH was intercalated with Keggin ion polyoxometalate K_4[α-$SiW_{12}O_{40}$] to form Ca/Al-[α-$SiW_{12}O_{40}$] as an effective adsorbent for iron(II) [23]. All results showed that LDH is an efficient material as an adsorbent of metal ions. Thus, research development of LDH is still conducted until this decade. As the brief researches as summaries before, the heavy metal ion in high level become toxic.

In this research, we conducted Ni/Cr and Ni/Cr-[α-$SiW_{12}O_{40}$] was used as adsorbent of iron(II) from an aqueous solution. To our best knowledge, iron is the fourth most essential element [24]. Fe(II) is required for proper transport and storage of oxygen by means of hemoglobin and myoglobin while its oxidized forms, methemoglobin and metmyoglobin, which contain Fe(III), will not bind oxygen [25]. Furthermore, iron (II) in high concentration, need to be decreasing because it is harmful and accumulated in the animal body [26]. Because of these findings, the way to remove Fe (II) is challenging the researcher to protect the environment. Materials Several factors of adsorption were studied, such as pHpzc, effect of adsorption time, effect of concentration of iron(II) and temperature, and also kinetic and thermodynamic properties were calculated based on experimental data.

2. Experimental

2.1. Chemicals and instrumentations

Chemicals are supplied from Merck and Sigma Aldrich, such as nickel(II) nitrate, chromium(III) nitrate, sodium hydroxide, sodium carbonate, sodium tungstate, sodium metasilicate, hydrochloric acid, and sodium chloride with pure analysis grade. Water was obtained from Purite® ion exchange water purification system at Universitas Sriwijaya. Nitrogen gas was supplied from a local supplier at Palembang, the capital city of South Sumatra, Indonesia. Characterization of X-ray analysis was conducted using XRD Rigaku Miniflex-600 with a scanning sample at 1 deg min^{-1}. Analysis of IR was carried out using FTIR Shimadzu Prestige-21 by KBr pellet. The sample was scanned at wavenumber 400–4000 cm^{-1}. Analysis of nitrogen adsorption-desorption was carried out using the Quantachrome apparatus at 77 K. Concentration of iron(II) was analyzed using UV-Vis BioBase BK-UV 1800 PC spectrophotometer after complexation with 1,10-phenanthroline at wavelength 510 nm. Keggin ion was synthesized according to previous literature [27].

2.2. Synthesis of Ni/Cr and Preparation of Ni/Cr-[α-$SiW_{12}O_{40}$] LDHs

Synthesis of Ni/Cr LDH was conducted by the coprecipitation method. Nickel(II) nitrate 0.3 M and chromium(III) nitrate 0.1 M were mixed with an equal amount with constant stirring. The solution of sodium hydroxide 1 M was added to the reaction mixture with an equal amount, and the pH of the reaction was adjusted to 10. The pH condition was arranged by the addition of or sodium hydroxide 0.1 M. The sodium carbonate solution 0.1 M was added after stable pH. The reaction was stirred for 17 h at 80 °C. The solid material was washed with water and dried at 110 °C overnight. The preparation of Ni/Cr-[α-$SiW_{12}O_{40}$] was carried

out using the ion-exchange method. The gel form of Ni/Cr was added with 5% $[\alpha\text{-}SiW_{12}O_{40}]^{4-}$. The mixtures were stirred for 24 h at room temperature under nitrogen conditions. The solid material was washed several times with water and dried at 110 °C overnight to form Ni/Cr-$[\alpha\text{-}SiW_{12}O_{40}]$ LDH.

2.3. Determination of pHpzc

Analysis of pH point zero charges (pzc) was carried out at various pH under sodium hydroxide or hydrochloric acid solution into the solution of sodium chloride 0.1 M. The pH solution of sodium chloride was adjusted in the range pH 1-10 by using hydrochloric acid 0.1 M or sodium hydroxide 0.1 M solutions. LDH of Ni/Cr or Ni/Cr-$[\alpha\text{-}SiW_{12}O_{40}]$ LDHs was added into the series of pH solution, then the solution mixtures were constantly stirred for 24 h. The solutions were filtered, and pH of the filtrate was determined by pH meter. The graph of pHpzc was obtained by comparison initial and final pH solution [28].

2.4. Adsorption studies

Adsorption of iron(II) on Ni/Cr and Ni/Cr-$[\alpha\text{-}SiW_{12}O_{40}]$ LDHs was carried out using a batch small reactor system. The adsorption process was used UV-vis spectrophotometer for determination the Fe(II) ion in an aqueous solution after complexation with 1,10-phenanthroline at a wavelength 510 nm. The complexation of Fe(II)-1,10-phenanthroline was studied by Tosonian et al. [29], as much as 5 ml of Fe(II) solution was added into 10 M HCl 2 ml in another beaker, the solution of 1,10-phenanthroline was dissolved by 10 mL HCl called ligand solution. Ligand solution was added dropwise into Fe(II) mixtures solution. The solution was added 10 ml buffer acetate 4.5. The solution was then shaken and allowed to stand for 30 min and then the absorbance was measured using a UV-Vis spectrophotometer at a wavelength of 450–560 nm. The adsorption study was studied through the effect of adsorption time, effect of iron(II) concentration, and temperature adsorption. Effect of adsorption time was investigated at various adsorption time i.e. 5, 10, 20, 30, 50, 60, 70, 90, 120, 150, 180 min. Effect of iron(II) concentration was varied at 30, 50, 60, 70 mg g^{-1} and at temperature 303, 313, 323, 333 K.

3. Results and discussion

The XRD powder patterns of Ni/Cr and Ni/Cr-$[\alpha\text{-}SiW_{12}O_{40}]$ LDHs are shown in Fig. 1. Ni/Cr LDH has a diffraction peak at 11.07° (003), 22.40° (006), 34.48° (009), and 60.43° (110) JCPDS file no. 38-0487 as a similar report by Ibrahimnova et al. [30]. The well-ordered formation of layer material was indicated at 11.07° (003) with an interlayer distance 7.99 Å. Intercalation of Ni/Cr with $[\alpha\text{-}SiW_{12}O_{40}]^{4-}$ ion to form Ni/Cr-$[\alpha\text{-}SiW_{12}O_{40}]$ LDH will shift the diffraction peak of (003) due to large ion exchange from nitrate to Keggin ion [31]. Ni/Cr-$[\alpha\text{-}SiW_{12}O_{40}]$ LDH has diffraction peak at 8.13° (003), 18.37° (006), 34.39° (009), 60.43° (110), and 61.65° (113). The diffraction at 8.13° (003) has an interlayer distance of 10.87 Å. Thus the intercalation process will increase the interlayer distance of LDH.

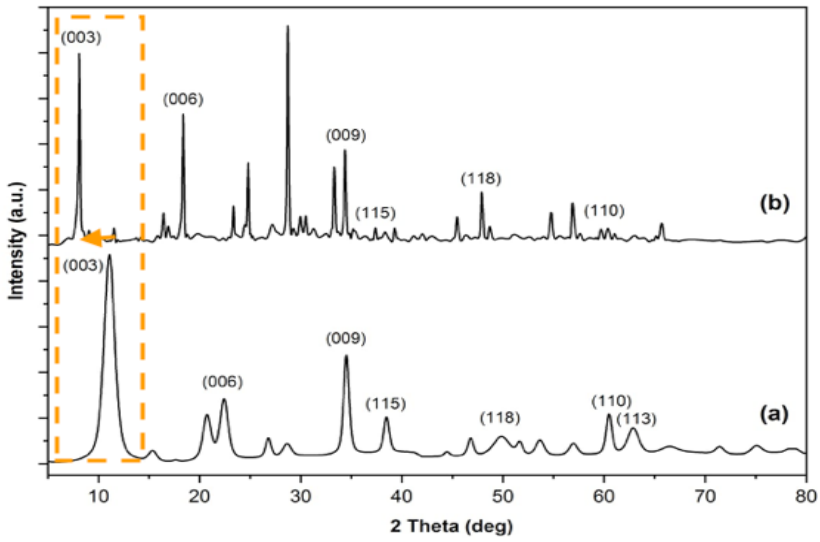

Fig. 1. XRD powder patterns of Ni/Cr (a) and Ni/Cr-$[\alpha\text{-}SiW_{12}O_{40}]$ (b) LDHs.

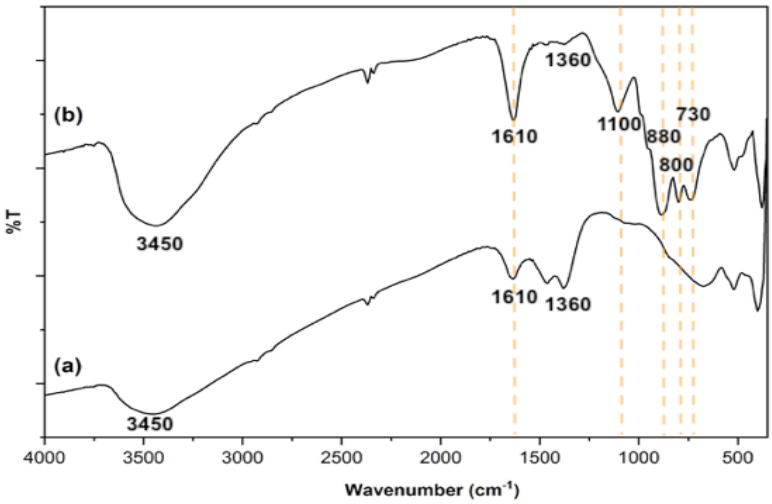

Fig. 2. FTIR spectra of Ni/Cr (a) and Ni/Cr-[α-$SiW_{12}O_{40}$] (b) LDHs.

The FTIR spectra of Ni/Cr and Ni/Cr-[α-$SiW_{12}O_{40}$] LDHs are shown in Fig. 2. Material Ni/Cr has three parts region i.e., water molecules vibration at 3450 cm^{-1}, the anion of nitrate and carbonate area at 1360–1610 cm^{-1}, and area of metal vibration at 600–750 cm^{-1} [29]. Intercalation of Ni/Cr with $[\alpha\text{-}SiW_{12}O_{40}]^{4-}$ ion resulting in significantly different IR spectra except for water molecules at 3450 cm^{-1}. The vibrations of anion nitrate and carbonate were changed to sharp one vibration at 1660 cm^{-1}, which was assigned as bending vibration of water molecules on the interlayer space of LDH. There were several vibration peaks at range 800–1100 cm^{-1} due to the vibration of Keggin ion (νW=O, νW-Oc-W, νW-Oe-W, and νSi-O) [32].

The isotherm adsorption-desorption of nitrogen on Ni/Cr and Ni/Cr-[α-$SiW_{12}O_{40}$] LDHs was shown in Fig. 3. The profile adsorption-desorption shows an H3 hysteresis loop on both Ni/Cr and Ni/Cr-[α-$SiW_{12}O_{40}$] LDHs at P/Po 0.89. The isotherm is categorized as a type IV isotherm model, and LDHs have mesoporous type materials [33].

The BET analysis of LDH, as shown in Table 1, indicating increase surface area of Ni/Cr to Ni/Cr-[α-$SiW_{12}O_{40}$] was equal with increasing interlayer distance of LDH as the data of XRD analysis. The pore volume was also increased after the intercalation process, caused that the layer of LDH's interlayer space was open due to intercalating wide anion. This phenom was also reported by [12] that LDH's interlayer space can be swelling according to intercalated anions.

The pHpzc analysis showed that the intersection point for Ni/Cr and Ni/Cr-[α-$SiW_{12}O_{40}$] was achieved at pH 7 and 9, respectively, as shown in Fig. 4. There are no charges of materials at the pHpzc point. The material will positively charge below the pHpzc value and vice versa. Thus adsorption of iron(II) will be conducted at pH 7 on Ni/Cr and pH 9 on Ni/Cr-[α-$SiW_{12}O_{40}$].

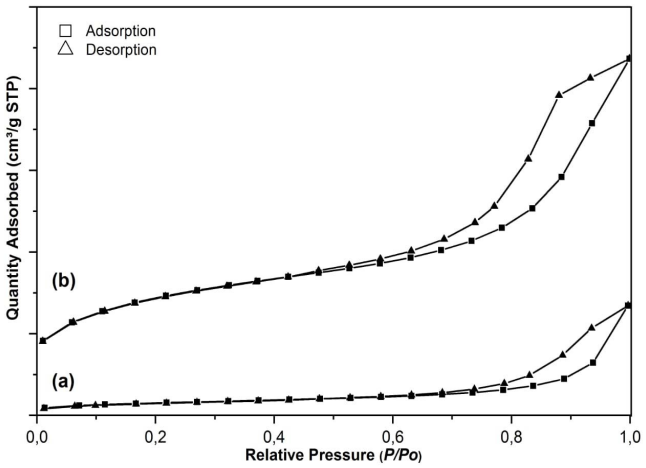

Fig. 3. The nitrogen adsorption desorption on Ni/Cr (a) and Ni/Cr-[α-$SiW_{12}O_{40}$] (b).

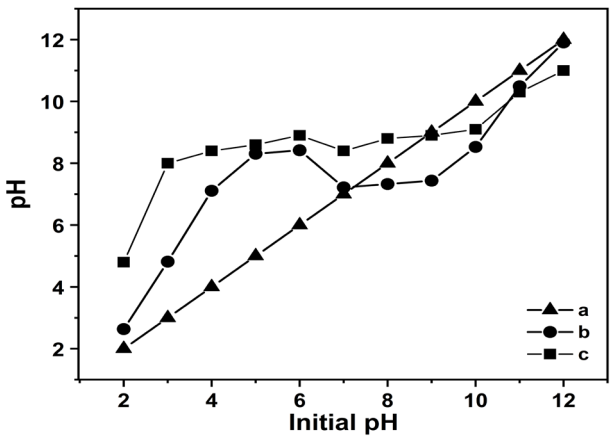

Fig. 4. pHpzc graph: initial pH (a), Ni/Cr (b) and Ni/Cr-[α-$SiW_{12}O_{40}$] (c).

Table 1
BET Analysis of LDH

Properties	LDHs	
	Ni/Cr	Ni/Cr-[α-$SiW_{12}O_{40}$]
BET Surface Area (m^2 g^{-1})	11.030	98.986
Pore volume (cm^3 g^{-1}), BJH	0.042	0.135
Pore diameter (nm), BJH	15.124	5.457

The adsorption of iron(II) was studied firstly through the effect of adsorption time, as shown in Fig. 5. The adsorption of iron(II) was increased with increasing adsorption time and reach equilibrium at the same time for both Ni/Cr and Ni/Cr-[α-$SiW_{12}O_{40}$] LDHs. The equilibrium was achieved at 70 min. Ni/Cr-[α-$SiW_{12}O_{40}$] LDH has a higher adsorption amount than Ni/Cr LDH at the same adsorption time.

The data of adsorption time was calculated using pseudo first-order and pseudo second-order [31] in Eqs. 1 and 2 to obtain the kinetic adsorption model, as shown in Table 2.

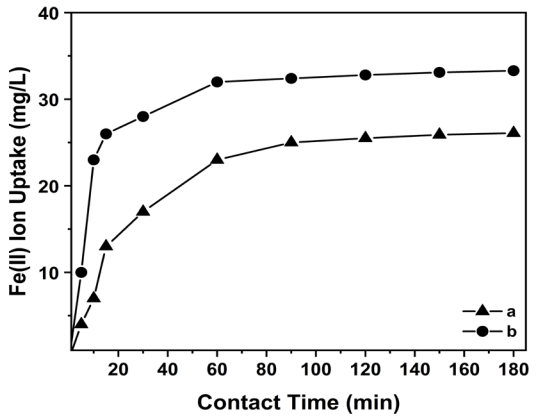

Fig. 5. Effect of adsorption time on Ni/Cr (a) and Ni/Cr-[α-$SiW_{12}O_{40}$] (b) LDHs.

Pseudo first-order kinetic model:

$$\log(q_e - q_t) = \log q_e - \left(\frac{k_1}{2.303}\right)t \quad (1)$$

where: q_e is adsorption capacity at equlibrium (mg g^{-1}); q_t is adsorption capacity at t (mg g^{-1}); t is adsorption time (minute); and k_1 is adsorption kinetic rate at pseudo first-order ($minute^{-1}$).

Pseudo second-order kinetic model:

$$\frac{t}{q_t} = \frac{1}{k_2 q_e^{\,2}} + \frac{1}{q_e}t \quad (2)$$

where q_e is adsorption capacity at equlibrium (mg g^{-1}); q_t is adsorption capacity at t (mg g^{-1}); t is adsorption time (minute); and k_2 is adsorption kinetic rate at pseudo second-order (g mg^{-1} $minute^{-1}$).

Table 2 showed that the adsorption process is followed pseudo second-order with R^2 is close to one. The k_1 and k_2 values indicate the constant adsorption rate for iron(II) on LDH. The k_2 value is higher than k_1 value shows adsorbent Ni/Cr-[α-$SiW_{12}O_{40}$] has higher reactivity toward iron(II) than adsorbent Ni/Cr. The effect of concentration of iron(II) and temperature adsorption is shown in Fig. 6.

Figure 6 showed that the adsorption of iron(II) was increased by increasing the concentration of iron(II). The adsorption of iron(II) on Ni/Cr-[α-$SiW_{12}O_{40}$] has higher than Ni/Cr for all temperature conditions. The amount of adsorption was slightly increased by increasing temperatures. The effect of temperature on the adsorption phenomena was indicated that the viscosity of the solvent, which iron(II) heavy metal ion has great mobility and the adsorption might be favorable at high temperatures. Isotherm adsorption can be obtained from data in Fig. 6 by using Freundlich and Langmuir isotherm

Table 2
Kinetic model adsorption of iron(II) on LDH

Kinetic Adsorption Model	Kinetic Parameter	LDH	
		Ni/Cr	Ni/Cr-[α-$SiW_{12}O_{40}$]
Pseudo First-Order	Qe_{Exp} (mg g^{-1})	135.274	172.260
	Qe_{Calc} (mg g^{-1})	121.899	127.057
	R^2	0.951	0.988
	k_1 (min^{-1})	0.0438	0.0507
Pseudo Second-Order	Qe_{Exp} (mg g^{-1})	135.274	172.260
	Qe_{Calc} (mg g^{-1})	166.667	200.000
	R_2	0.996	0.998
	k_2 (g $mg^{-1}min^{-1}$)	0.0002	0.0006

models, as shown in Eqs. 3 and 4 as similarly reported by Siregar et al. [34]. The isotherm adsorption of iron(II) on LDH was presented in Table 3.

Langmuir equation:

$$\frac{C}{m} = \frac{1}{bK} + \frac{C}{b} \quad (3)$$

where C is a saturated concentration of adsorbate; m is the amount of adsorbate; b is the maximum adsorption capacity (mg g^{-1}), and K_{ML} is the Langmuir constant (L mg^{-1}).

Freundlich equation:

$$\log q_e = \log K_F + 1/n \log C_e \quad (4)$$

where q_e is adsorption capacity at equilibrium (mg g^{-1}); C_e is the concentration of adsorbate at equilibrium (mg L^{-1}), and K_F is Freundlich constant.

Adsorption of iron(II) on LDH follows the Langmuir isotherm model for all temperature conditions indicated that adsorption of iron(II) on LDH was monolayer adsorption process. The adsorption capacity of iron(II) on Ni/Cr-[α-$SiW_{12}O_{40}$] was up to 250 mg g^{-1}. Then adsorbent Ni/Cr-[α-$SiW_{12}O_{40}$] is potential adsorbent for removal heavy metal from aqueous solution.

The thermodynamic parameter as shown in Table 4 was obtain using thermodynamic Eqs. 5–6.

$$\ln K_{ML} = \frac{\Delta S}{R} - \frac{\Delta H}{RT} \quad (5)$$

$$\Delta G^{\circ} = -RT \ln K_{ML} \quad (6)$$

where T is the temperature (K); R is the gas constant (8.314 J mol^{-1} K^{-1}), and K_{ML} is the modified

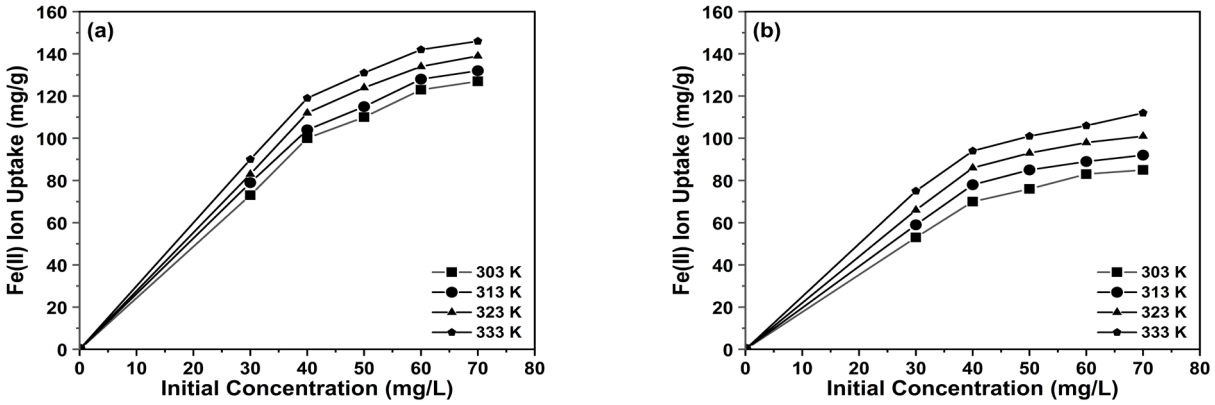

Fig. 6. Effect of iron(II) concentration and temperature adsorption on Ni/Cr (a) and Ni/Cr-[α-$SiW_{12}O_{40}$] (b) LDHs.

Table 3
Isotherm adsorption of iron (II) on LDH

Ni/Cr	Isotherm	Isotherm Parameter	Temperature (K)			
			303	313	323	333
Langmuir	Langmuir	q_{max} (mg g^{-1})	166.667	200.000	200.000	200.000
		k_{ML} (L mg^{-1})	0.035	0.033	0.036	0.035
		R^2	0.811	0.865	0.891	0.921
	Freundlich	k_F (mg g^{-1})(L $mg)^{1/n}$	13.397	15.417	16.943	15.922
		n	1.862	1.931	1.972	1.852
		R^2	0.748	0.787	0.808	0.882
Ni/Cr-[α-$SiW_{12}O_{40}$]	Langmuir	q_{max} (mg g^{-1})	250.000	250.000	250.000	250.000
		K_{ML} (L mg^{-1})	0.036	0.039	0.043	0.048
		R^2	0.974	0.988	0.993	0.995
Ni/Cr-[α-$SiW_{12}O_{40}$]	Freundlich	k_F (mg g^{-1})(L $mg)^{1/n}$	21.135	22.909	25.704	28.576
		n	1.996	2.041	2.137	2.247
		R^2	0.944	0.966	0.972	0.970

Table 4
Thermodynamic parameter

LDH	ΔGo (kJ mol^{-1})				ΔH^o (kJ mol^{-1})	ΔS^o (J mol^{-1} K^{-1})
	303 K	313 K	323 K	333 K		
Ni/Cr	-1.723	-2.016	-2.309	-2.602	7.149	0.029
Ni/Cr-[α-$SiW_{12}O_{40}$]	-2.822	-3.059	-3.295	-3.532	4.354	0.024

Langmuir constant. The modified Langmuir constant was obtained from Table 3. The data in Table 4 show adsorption of iron(II) on Ni/Cr and Ni/Cr-[α-$SiW_{12}O_{40}$] LDHs have ΔH^o values in the range 4.354–7.149 kJ mol^{-1}. That energy is classifying as physical energy adsorption. The negative values of ΔG^o for all temperature conditions showed that adsorption of iron(II) on LDH was a spontaneous process. The negative value of ΔS^o shows to increase in the randomness of the adsorption process between iron(II) and LDHs.

4. Conclusion

Ni/Cr LDH was successfully synthesized via a facile coprecipitation method under alkaline conditions. Further modification of the synthesized Ni/Cr-[α-$SiW_{12}O_{40}$] was successfully performed by intercalating by Keggin ion $SiW_{12}O_{40}^{4-}$ with Ni/Cr-LDH. The success of the intercalation was confirmed by the increase in the interlayer space or interlayer gallery and increasing the surface area. The surface area of LDH after intercalation was increased from 11.030 to 98.986 m^2 g^{-1} equal with an increasing interlayer distance of LDH from 7.99 to 10.87 Å. Adsorption of iron(II) on Ni/Cr-[α-$SiW_{12}O_{40}$] LDH were categorized as physical adsorption with an adsorption capacity is up to 250 mg g^{-1}. Thus Ni/Cr-[α-$SiW_{12}O_{40}$] is a potential adsorbent for removal iron(II) from aqueous solution.

Acknowledgement

This research was supported by Hibah Profesi in fiscal year 2019/2020 from Universitas Sriwijaya contract No. 0014/UN9/SK.LP2M.PT/2019. The authors also thank the Research Center of Inorganic Materials and Coordination Complexes, Faculty of Mathematics, and Natural Sciences Universitas Sriwijaya for laboratory facilities.

References

[1]. M. Daud, A. Hai, F. Banat, M.B. Wazir, M. Habib, G. Bharath, M.A. Al-Harthi, *J. Mol. Liq.* 288 (2019) 110989. DOI: 10.1016/j.molliq.2019.110989

[2]. Y. Lu, B. Jiang, L. Fang, F. Ling, J. Gao, Fang Wu, Xihua Zhang, *Chemosphere* 152 (2016) 415–422. DOI: 10.1016/j.chemosphere.2016.03.015

[3]. J.D. Castro-Castro, I.F. Macías-Quiroga, G.I. Giraldo-Gómez, N.R. Sanabria-González, *Sci. World J.* 2020, ID 3628163. DOI: 10.1155/2020/3628163

[4]. L.N.H. Arakaki, V.L.S. Augusto Filha, K.S. de Sousa, F.P. Aguiar, M.G. da Fonseca, J.G.P. Espínola, *Thermochim. Acta* 440 (2006) 176–180. DOI: 10.1016/j.tca.2005.11.004

[5]. N. Kataria, V.K. Garg, *J. Mol. Liq.* 271 (2018) 228–239. DOI: 10.1016/j.molliq.2018.08.135

[6]. N.R. Palapa, T. Taher, A. Wijaya, A. Lesbani, *Science and Technology Indonesia* 6 (2021) 209–217. DOI: 10.26554/sti.2021.6.3.209-217

[7]. R. Kumar, M.A. Laskar, I.F. Hewaidy, M.A. Barakat, *Earth Syst. Environ.* 3 (2019) 83–93. DOI: 10.1007/s41748-018-0085-3

[8]. S.Y. Cheng, P.L. Show, B.F. Lau, J.S. Chang, T.C. Ling, *Trends Biotechnol.* 37 (2019) 1255–1268. DOI: 10.1016/j.tibtech.2019.04.007

[9]. L.M. Estiaty, *Indonesian Journal of Geology and Mining* 22 (2012). DOI: 10.14203/risetgeotam2012.v22.63

[10]. H. Zhou, Z. Jiang, S. Wei, *Appl. Clay Sci.* 153 (2018) 29–37. DOI: 10.1016/j.clay.2017.11.033

[11]. Q.Ul Ain, H. Zhang, M. Yaseen, U. Rasheed, K. Liu, S. Subhan Z. Tong, *J. Clean. Prod.* 247 (2020) 119088. DOI: 10.1016/j.jclepro.2019.119088

[12]. S. Samuei, F.A. Rad, Z. Rezvani, *Appl. Clay Sci.* 184 (2020) 105388. DOI: 10.1016/j.clay.2019.105388

[13]. S. Ma, J. Wang, L. Du, Y. Sun, Q. Gu, G. Sun, X. Yang, *J. Colloid Interf. Sci.* 393 (2013) 29–35. DOI: 10.1016/j.jcis.2012.10.015

[14]. X. Duan, J. Lu, D.G. Evans, Modern Inorganic Synthetic Chemistry 2011, 375–404. DOI: 10.1016/B978-0-444-53599-3.10017-4

[15]. M.J. Barnabas, S. Parambadath, A. Mathew, S.S. Park, A. Vinu, C.-S. Ha, *J. Solid State Chem.* 233 (2016) 133–142. DOI: 10.1016/j.jssc.2015.10.001

[16]. L. Ma, Q. Wang, S.M. Islam, Y. Liu, S. Ma, M.G. Kanatzidis, *J. Am. Chem. Soc.* 138 (2016) 2858–2866. DOI: 10.1021/jacs.6b00110

[17]. B. Ou, J. Wang, Y. Wu, S. Zhao, Z. Wang, *Chem. Eng. J.* 380 (2020) 122600. DOI: 10.1016/j.cej.2019.122600

[18]. M. Laipan, H. Fu, R. Zhu, L. Sun, J. Zhu, H. He, *Sci. Rep.* 7 (2017) 7277. DOI: 10.1038/s41598-017-07775-8

[19]. M. Huang, Y. Zhang, W. Xiang, T. Zhou, X. Wu, J. Mao, *J. Environ. Sci.-China* 85 (2019) 56–65. DOI: 10.1016/j.jes.2019.04.011

[20]. S. Sasaki, S. Aisawa, H. Hirahara, A. Sasaki, H. Nakayama, E. Narita, *J. Eur. Ceram. Soc.* 26 (2006) 655–659. DOI: 10.1016/j.jeurceramsoc.2005.06.021

[21]. M. Oktriyanti, N.R. Palapa, A. Lesbani, *J. Ecol. Eng.* 21 (2020) 63–71. DOI: 10.12911/22998993/122190

[22]. W. Tian, X. Kong, M. Jiang, X. Lei, X. Duan, *Mater. Lett.* 175 (2016) 110–113. DOI: 10.1016/j.matlet.2016.03.141

[23]. T. Taher, M.M. Christina, M. Said, N. Hidayati, F. Ferlinahayati, A. Lesbani, *Bull. Chem. React. Eng. Catal.* 14 (2019) 260–267. DOI: 10.9767/bcrec.14.2.2880.260-267

[24]. M.A. de Bittencourt, A.M. Novack, J.A. Scherer Filho, L.P. Mazur, B.A. Marinho, A. da Silva, A.A. U. de Souza, S.M.A. Guelli U. de Souza, *J. Clean. Prod.* 268 (2020) 122164. DOI: 10.1016/j.jclepro.2020.122164

[25]. W.S.W. Ngah, S. Ab Ghani, A. Kamari, *Bioresource Technol.* 96 (2005) 443–450. DOI: 10.1016/j.biortech.2004.05.022

[26]. A. Lesbani, N. Normah, N.R. Palapa, T. Taher, R. Andreas, R. Mohadi, *Molekul* 15 (2020) 149–157. DOI: 10.20884/1.jm.2020.15.3.600

[27]. Y. Hanifah, N.R. Palapa, *Sci. Technol. Indones.* 1 (2016) 16–19. DOI: 10.26554/sti.2016.1.1.16-19

[28]. A. Lesbani, H. Hensen, T. Taher, N. Hidayati, R. Mohadi, R. Andreas, *AIP Conf. Proc.* 2026 (2018) 020011. DOI: 10.1063/1.5064971

[29]. S. Tosonian, C.J. Ruiz, A. Rios, E. Frias, J.F. Eichler, *Open Journal of Inorganic Chemistry* 3 (2013) 7–13. DOI: 10.4236/ojic.2013.31002

[30]. K.A. Ibrahimova, A.A. Azizov, O.O. Balayeva, R.M. Alosmanov, S.C. Mammadyarova, *Mendeleev Commun.* 31 (2021) 100–103. DOI: 10.1016/j.mencom.2021.01.031

[31]. N.R. Palapa, N. Juleanti, N. Normah, T. Taher, A. Lesbani, *Bull. Chem. React. Eng. Catal.* 15 (2020) 653–661. DOI: 10.9767/bcrec.15.3.8371.653-661

[32]. T. Taher, Y. Irianty, R. Mohadi, M. Said, R. Andreas, A. Lesbani, *Indones. J. Chem.* 19 (2019) 873–881. DOI: 10.22146/ijc.36447

[33]. G. Zhao, L. Liu, C. Li, T. Zhang, T. Yan, J. Yu, X. Jiang, F. Jiao, *J. Photochem. Photobiol. A Chem.* 367 (2018) 302–311. DOI: 10.1016/j.jphotochem.2018.08.048

[34]. P.M.S.B.N. Siregar, N.R. Palapa, A. Wijaya, E.S. Fitri, A. Lesbani, *Sci. Technol. Indones*. 6 (2021) 85–95. DOI: 10.26554/sti.2021.6.2.85-95